Magnetic, calorimetric, and transport properties of $Ce(Pd_{1-x}Ni_x)_2Ge_2$ and $CeNi_2(Ge_{1-y}Si_y)_2$

G. Knebel, M. Brando, J. Hemberger, M. Nicklas, W. Trinkl, and A. Loidl
Experimentalphysik V, Elektronische Korrelationen und Magnetismus, Institut für Physik, Universität Augsburg, D-86159 Augsburg, Germany

(Received 8 October 1998; revised manuscript received 21 January 1999)

We present results of a systematic study of the isoelectronic Kondo-lattice compounds $Ce(Pd_{1-x}Ni_x)_2Ge_2$ and $CeNi_2(Ge_{1-y}Si_y)_2$. With increasing x and y the hybridization of the localized $4f$ moments with the band states increases. Consequently the magnetic order of the Pd-rich compounds becomes suppressed, yielding a heavy-fermion behavior in $CeNi_2Ge_2$, and an intermediate valence state in Si-rich alloys. The electrical resistivity, magnetic susceptibility, and specific heat were investigated for temperatures $0.1<T<300$ K. The antiferromagnetic order of localized spins in $Ce(Pd_{1-x}Ni_x)_2Ge_2$ diminishes for $x\geqslant 0.9$ and intermediate valent behavior evolves for $y\geqslant 0.3$. We find significant deviations from Fermi-liquid behavior in a broad concentration range, which extends from $x=0.9$ into the intermediate valence regime ($y=0.4$). The results are compared with model predictions for magnetic systems close to a quantum critical point and for systems with frozen-in magnetic disorder (Griffiths phase). And although we find qualitatively the fingerprints of a quantum critical point, resistivity and heat capacity cannot be explained coherently within the same model. [S0163-1829(99)00219-2]

I. INTRODUCTION

The ground-state properties of heavy-fermion systems (HFS) are crucially determined by the competition of the Kondo- and the Ruderman-Kittel-Kasuya-Yosida (RKKY)-energy scales.[1,2] The formation of local Kondo singlets depends exponentially on the exchange interaction J, $T_K \propto \exp(N_F J)$, while the formation of long-range order of localized magnetic moments depends quadratically on J, $T_{RKKY} \propto (N_F J)^2$.[3] $N_F J$ is a dimensionless effective exchange-coupling constant between local magnetic moments and conduction electrons with density N_F at the Fermi level. At small values of $N_F J$ local-moment magnetism (LMM) is dominating. For large values intermediate-valence (IV) phenomena are expected. It is just at the borderline from the IV regime to LMM where heavy-fermion (HF) behavior is expected, including HF superconductivity and HF-band magnetism.

In recent years this transition region from magnetic order to a nonmagnetic ground state has found renewed interest due to the appearance of non-Fermi-liquid (NFL) phenomena. (for a recent review, see Ref. 4). The characteristics of NFL behavior are an electrical resistivity that can be described by $\rho=\rho_0+A'T^n$ with $n<2$ (the exponent $n=2$ is characteristic for electron-electron interactions in the framework of the Fermi-liquid theory), a temperature-dependent magnetic susceptibility for $T\rightarrow 0$ K, in contrast to a temperature-independent Pauli-spin susceptibility and a specific-heat coefficient of the specific heat which usually reveals roughly a logarithmic divergence when approaching the lowest temperatures. Theoretically NFL behavior has been described within multichannel Kondo models[5,6] and using a concept of a distribution of Kondo temperatures.[7,8] The appearance of NFL behavior has also been predicted in the vicinity of a magnetic $T=0$ K phase transition,[9–11] which marks a quantum-critical point (QCP) and in disordered systems in terms of the Griffiths phase[12] which is a cluster model of a spin-glass phase.[13]

The aim of this work is to change, via isoelectronic chemical substitutions, the hybridization strength and to pass continuously from a system with LMM to the IV regime, paying special attention to the critical concentration where magnetism is completely suppressed. For this investigation we chose the ternary alloys $Ce(Pd_{1-x}Ni_x)_2Ge_2$ and $CeNi_2(Ge_{1-y}Si_y)_2$, which crystallize in the $ThCr_2Si_2$ structure. $CePd_2Ge_2$ is a local-moment magnet with an antiferromagnetic (AFM) phase transition temperature of $T_N=5.1$ K. The size of the ordered moment, $\mu_s=1.79\mu_B$, shows that moment compensation plays a minor role.[14] $CeNi_2Ge_2$ is a nonmagnetic HFS with a characteristic Kondo-lattice temperature $T^*=40$ K, characterized by a specific-heat coefficient $\gamma=350$ mJ/mole K^2.[15,16] The phase diagram of the $Ce(Pd_{1-x}Ni_x)_2Ge_2$ system was recently also studied by Fukuhara *et al.*[17] Finally, $CeNi_2Si_2$ is an IV system with a characteristic temperature in the order of 600 K.[18] By chemical substitution the volume decreases from approximately 190 $Å^3$ (95 $Å^3$ volume per one Ce ion) from the magnetic $CePd_2Ge_2$ by almost 20% to 155 $Å^3$ (78 $Å^3$/Ce) in intermediate valent $CeNi_2Si_2$, thereby increasing the hybridization strength considerably.

We performed systematic magnetic susceptibility, electrical resistivity, and specific-heat experiments for temperatures 0.1–400 K and in magnetic fields up to 160 kOe. Besides an investigation of the systematic evolution of the calorimetric, magnetic, and transport properties with increasing hybridization, we wanted to focus especially on the transition region from LMM to Kondo behavior searching for NFL effects. A detailed report on the field dependent properties of these alloys will be given in a forthcoming paper.

II. SAMPLE PREPARATION AND CHARACTERIZATION

The samples were prepared by repeated arc melting of the appropriate quantities of the pure constituent elements in argon atmosphere. After melting, the samples were annealed at

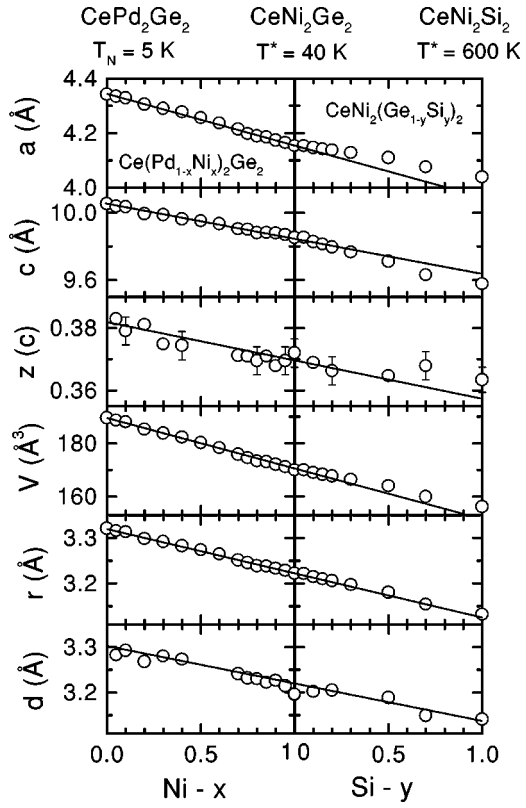

FIG. 1. Lattice parameters *a*, *c*, and *z*, volume *V*, Ce transition-metal distance *r* and Ce-(Si,Ge) distance *d* as a function of nickel concentration *x* and silicon concentration *y*. Error bars are indicated in $z(x,y)$. The errors are smaller than the symbols for *a*, *c*, *V*, *r*, and *d*. The solid lines represent linear extrapolations of these parameters from the regime of a stable Ce^{3+} valence ($0<x<0.8$) into the intermediate valence regime (large *y*).

800 °C for 100 h. Microprobe and x-ray powder-diffraction techniques confirmed the specimens to be single phase and to crystallize in the proper body-centered tetragonal $ThCr_2Si_2$ structure.

The lattice constants *a* and *c*, as well as the volume *V* and the distance *r* of the Ce ion from the transition metal, have been determined from the positions of the Bragg reflections of the powder pattern. The *z* parameters (which is a free parameter in the $ThCr_2Si_2$ structure) were determined from an analysis of the intensities of the diffraction pattern. Using this *z* parameter we calculated also the distance *d* from the Ce ion to the Si (or Ge) atoms. It has been speculated that the increasing hybridization is not purely a volume effect but depends crucially on the hybridization with the electron densities of neighboring ions.[18] Figure 1 shows the concentration dependence of the lattice parameters, of the volume, and of the interatomic distances *r* and *d* for all compositions. The solid lines in Fig. 1 indicate a linear extrapolation (Vegard's rule) from the Pd-rich to the Si-rich alloys. It becomes immediately clear that *a*, *c*, and *z* reveal significant deviations from linearity for concentrations where IV behavior is observed. This for a lesser degree is also true for the volume. But the Ce-transition metal distance *r* and the Ce-Si (Ge) distance *d*, both closely follow Vegard's law for all concentrations. It is also interesting to note that the value of *r* and *d* are almost equal for all concentrations.

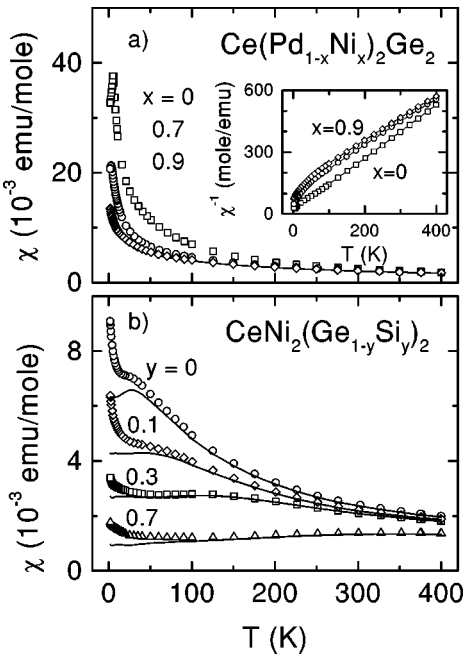

FIG. 2. Magnetic susceptibility vs temperature in $Ce(Pd_{1-x}Ni_x)_2Ge_2$ (upper panel) and $CeNi_2(Ge_{1-y}Si_y)_2$ (lower panel). The solid lines were calculated assuming a Curie law due to an amount of 1% free Ce^{3+} impurities. For $x=0.9$, in the upper panel the solid line is within the symbols even at the lowest temperatures. The inset in (the upper panel) shows χ^{-1} vs temperature for $x=0$, 0.7, and 0.9.

III. EXPERIMENTAL RESULTS

A. Magnetic susceptibility

The magnetic susceptibility was studied using a superconducting quantum interference device (SQUID) magnetometer (Quantum Design) which operates from 1.8–400 K in magnetic fields up to 70 kOe and an Oxford ac susceptometer which allows measurements from 1.4–300 K in fields up to 160 kOe. The dc susceptibility, $\chi_{dc}=M/H$, of a representative number of compounds is shown in Fig. 2. These measurements were performed in the SQUID magnetometer in an external field of 5 kOe. In the temperature window of the dc experiments ($T>1.8$ K) magnetic order can be observed for Ni concentrations $x<0.8$. As will be seen later, magnetic order is fully suppressed close to $x=0.9$. This value will be treated as critical concentration x_c in the following.

On the Si-rich side, where the IV regime is entered and the low-temperature susceptibility is low, a small upturn of the susceptibility at the lowest temperature most probably is due to a small amount of magnetic defects. The solid line was calculated assuming approximately 1% of free Ce $4f^1$ spins. This free-spin contribution is clearly seen in compounds which reveal Pauli paramagnetism at low temperatures but is negligible in the Pd:Ni alloys. For $x=0.9$ the corrected susceptibility (solid line) is within the size of the symbols of the raw data. For $x\leqslant 0.7$ a sharp anomaly indicates the transition into an AFM phase at low temperatures. The magnetic structures so far have not been determined. For concentrations $y>0.1$, a weak maximum in $\chi(T)$ is a characteristic signature of spin (or valence) fluctuations. The temperature of the maximum susceptibility can be read off as characteristic temperature T^*.

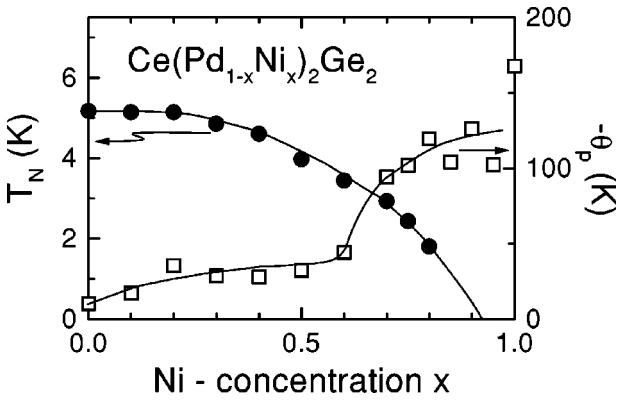

FIG. 3. The antiferromagnetic ordering temperatures T_N (left scale) and the paramagnetic Curie-Weiss temperatures θ_p (left scale) in $Ce(Pd_{1-x}Ni_x)_2Ge_2$ as a function of Ni concentration x.

The inverse susceptibility is shown as the inset in Fig. 2. From χ^{-1} vs T we determined the paramagnetic moments and the Curie-Weiss temperatures θ_p. All compounds reveal a high-temperature paramagnetic moment of approximately $(2.6\pm0.1)\mu_B$ close to the value of the full Ce moment (2.54 μ_B). The Curie-Weiss temperature weakly depends on the nickel concentration for $x<0.6$ and strongly increases on further increasing x, an effect that will be discussed later in detail and which is characteristic for IV systems. The characteristic temperatures T_N and θ_p as a function of the Ni concentration are shown in Fig. 3. The critical concentration between AFM order and a non-magnetic ground state is close to $x=0.9$. The paramagnetic Curie-Weiss temperature is between 15 and 45 K for $x<0.6$ and increases towards 150 K for pure $CeNi_2Ge_2$. These findings are in close agreement with Ref. 17. However, it is interesting to note that when Ge is substituted by Si in $CePd_2Ge_2$, the Néel temperature increases linearly from $T_N\approx5$ K to $T_N\approx10$ K.[19] Pressure studies of the Néel temperature of $CePd_2Ge_2$ show a linear increase of T_N with increasing pressure, too.[20]

B. Resistivity

The temperature and magnetic-field dependence of the electrical resistivity has been measured by conventional four-point techniques for temperatures $0.06<T<300$ K. Representative results for $Ce(Pd_{1-x}Ni_x)_2Ge_2$ (upper panel) and $CeNi_2(Ge_{1-y}Si_y)_2$ (lower panel) are shown in Fig. 4. With decreasing temperature and for the palladium-rich samples a single-ion Kondo minimum and a concomitant Kondo increase towards low temperatures is followed by a steep decrease due to the magnetic phase transitions and the onset of coherence effects of the Kondo lattice. With increasing Ni concentration x the temperature of the Kondo minimum shifts almost linearly from $T=15$ K ($x=0$) to $T=30$ K ($x=0.8$). The low-temperature maximum decreases from $T\approx5.2$ K for $x=0$ to $T\approx4.2$ K for $x=0.7$ and is located just above the Néel temperature. It is influenced by the suppression of disorder scattering due to AFM short-range order just above T_N. In the region where $T_N\rightarrow0$ K the maximum is shifted to higher temperatures and defines the coherence maximum of the Kondo lattice which corresponds to the Kondo lattice temperature T^*. The inset in Fig. 4 shows the magnetic contribution to the resistivity for $CePd_2Ge_2$ derived

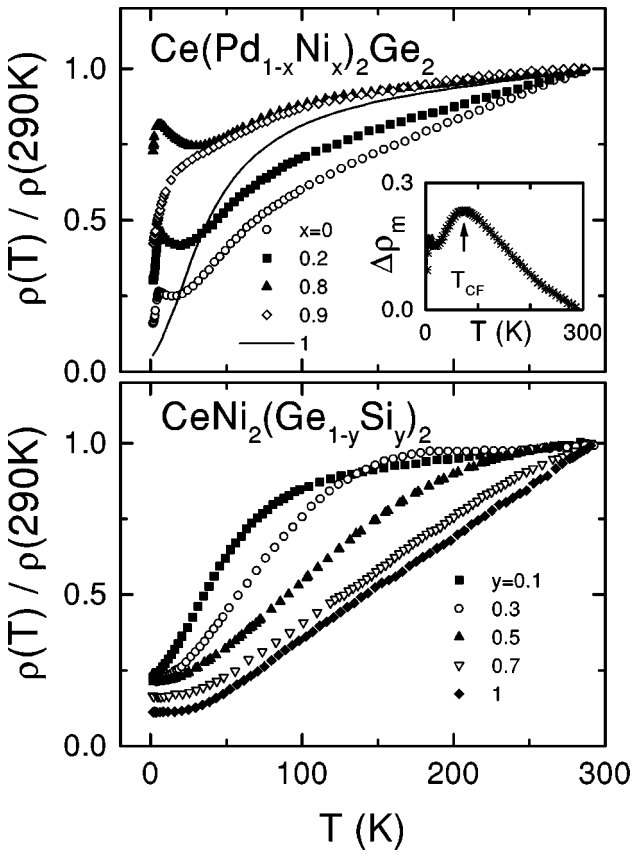

FIG. 4. The temperature dependence of the resistivity for a series of concentrations in $Ce(Pd_{1-x}Ni_x)_2Ge_2$ (upper panel) and $CeNi_2(Ge_{1-y}Si_y)_2$ (lower panel). The resistivity has been normalized at room temperature. The inset in the upper frame shows the magnetic contribution of the resistivity for $CePd_2Ge_2$ determined by subtracting the resistivity of $LaPd_2Ge_2$.

by subtracting the resistivity of $LaPd_2Ge_2$. The second maximum (located roughly at 75 K), certainly is due to crystal electric-field (CEF) effects. The character of the electrical transport changes significantly at $x=0.9$. While the sample with a nickel concentration of $x=0.8$ still reveals the characteristics of a magnetically ordered Kondo system, for $x=0.9$ $\rho(T)$ shows the typical heavy-fermion behavior with a relatively high characteristic temperature [e.g., like UPt_3 (Ref. 21)] where the coherence maximum is already suppressed and the coherence peak and the CEF peak have merged into one broad shoulder. That this is not an effect of disorder can be clearly seen in the pure $CeNi_2Ge_2$ compound which reveals a similar behavior. In this compound the magnetic relaxation rate, as observed in neutron-scattering experiments, indicates a characteristic temperature $T^*=40$ K.[15,16] The lower panel of Fig. 4 demonstrates how the broad Kondo enhancement with increasing hybridization (increasing Si concentration y) is shifted to higher temperatures. $CeNi_2Si_2$ reveals an almost normal metallic behavior below room temperature. The low temperature ($0.1<T<2.5$ K) behavior of the resistance is shown in Fig. 5. To show possible deviations from a pure Fermi-liquid behavior we plotted the resistance ρ vs T^2. Figure 5 clearly shows FL behavior of the resistivity only for the compound with $y=0.3$. Significant deviations appear in the magnetically ordered phase ($x=0.6$) and for the compounds just at the borderline from magnetic order to the pure Kondo regime. An upward cur-

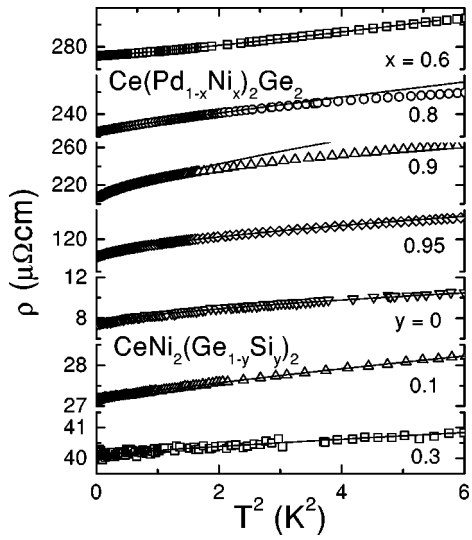

FIG. 5. Low-temperature part of the resistivity in $Ce(Pd_{1-x}Ni_x)_2Ge_2$ and $CeNi_2(Ge_{1-y}Si_y)_2$ for some selected concentrations as a function of T^2. The solid lines are fits to a function as described in the text.

vature of ρ vs T^2 indicates a temperature exponent $n>2$ for the antiferromagnetic compound, while for $x=0.8$, 0.9, 0.95 as well as for $y=0$ and 0.1 a downward curvature signals exponents $n<2$. The detailed analysis will be discussed later. In Fig. 6 the cross section for quasiparticle-quasiparticle scattering measured by $A(T)=[\rho(T)-\rho_0]/T^2$ is potted as a function of temperature. Just at the critical concentration and towards low temperatures, $A(T)$ reveals a divergence instead of remaining constant as expected for a Fermi liquid. Figure 6 provides a clear indication of the anomalous scattering observed in the NFL regime.

C. Heat capacity

The temperature-dependent heat capacity was determined with a standard quasiadiabatic method in an Oxford ^{4}He cryostat for temperatures $2.5<T<25$ K and using a relaxation method in an Oxford ^{3}He cryostat for $0.3<T<5$ K. Some representative results of the heat capacity, plotted as

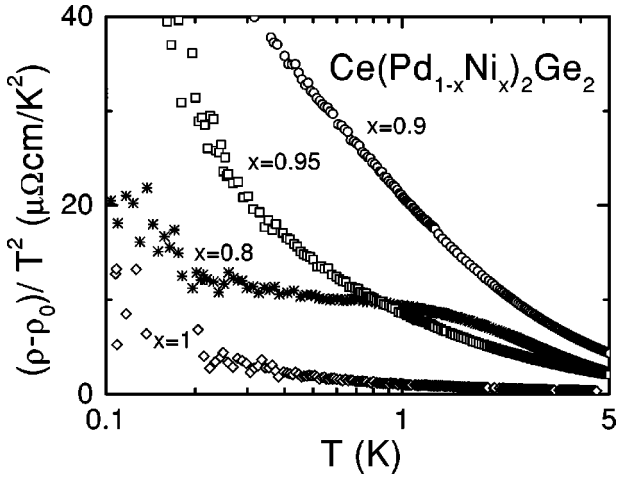

FIG. 6. Quasiparticle-quasiparticle cross section $A=[\rho(T)-\rho_0]/T^2$ vs T for Ni concentrations close to the critical regime.

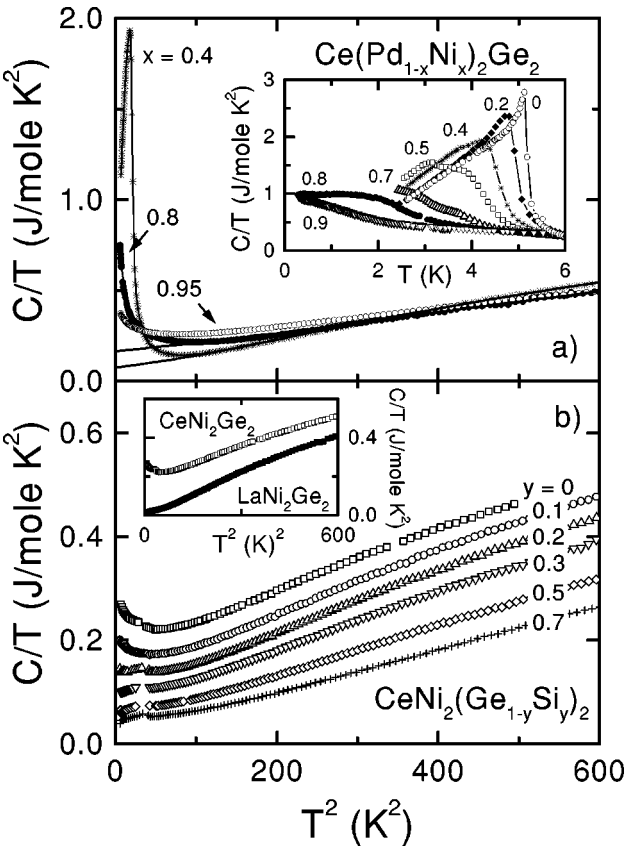

FIG. 7. Heat capacity in $Ce(Pd_{1-x}Ni_x)_2Ge_2$ (upper panel) and $CeNi_2(Ge_{1-y}Si_y)_2$ (lower panel) plotted as C/T vs T^2. The inset in upper panel shows the low-temperature heat capacity for a series of Ni concentrations $0\leqslant x\leqslant 0.9$. The inset in the lower panel compares the heat capacity of $CeNi_2Ge_2$ with the reference compound $LaNi_2Ge_2$.

C/T vs T^2 are shown in Fig. 8. The $Ce(Pd_{1-x}Ni_x)_2Ge_2$ system is shown in the upper panel of Fig. 7 and demonstrates that with increasing x, the magnetic phase transition is shifted to lower temperatures (inset in upper panel of Fig. 7). A double peak structure of the specific heat can be seen for the concentrations $x\geqslant 0.5$. This might be due to a change of the magnetic structure in this regime. Other AFM systems also reveal similar double peak structures in the specific heat.[23,24] Finally, for $x=0.9$ and 0.95 the alloys remain paramagnetic down to the lowest temperatures. In $CeNi_2Ge_2$ the specific-heat coefficient γ still reveals a significant increase towards $T=0$ K (Fig. 7, lower panel). The inset in the lower panel of Fig. 7 shows C/T of $CeNi_2Ge_2$ in comparison to the reference compound $LaNi_2Ge_2$. With increasing hybridization (increasing y) this low-temperature enhancement and deviation from Fermi-liquid behavior vanishes. For $y=0.7$ a pure Fermi-liquid behavior can be observed down to the lowest temperatures with a constant specific-heat coefficient of approximately 50 mJ/mole K^2.

The temperature dependence of the specific-heat coefficient, around the critical concentration where magnetic behavior is suppressed, is shown in Fig. 8. To demonstrate the clear NFL behavior, at least in limited temperature regimes, we plotted C/T vs $\log(T)$. By subtracting the low-temperature heat capacity of pure $LaNi_2Ge_2$ we determined only the $4f$ derived contributions to $C(T)$. A logarithmic

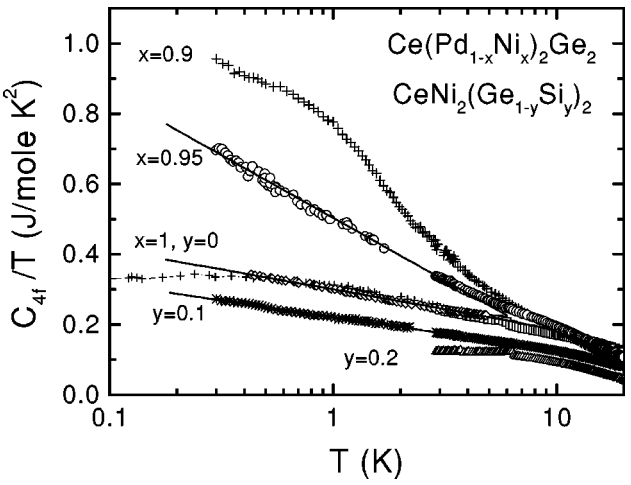

FIG. 8. The $4f$-derived heat capacity for concentrations close to the critical concentration in $Ce(Pd_{1-x}Ni_x)_2Ge_2$ and $CeNi_2(Ge_{1-y}Si_y)_2$ plotted as C/T vs $\log(T)$. The ''NFL'' behavior $C/T \propto \log(T)$ is indicated as solid line for the different concentrations. [Data for $CeNi_2Ge_2$ at low temperatures were taken from Ref. 15 (+) and Ref. 31 ($\diamond$).]

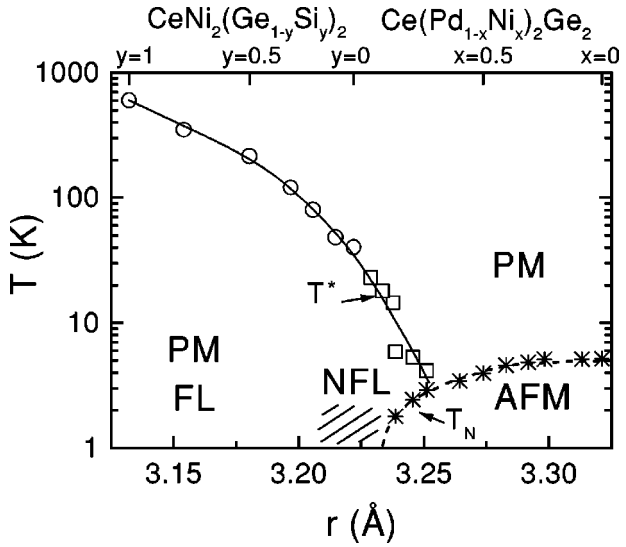

FIG. 9. Characteristic temperatures T^* and T_N vs the Ce transition-metal distance r. The solid lines are drawn to guide the eye. The shaded area indicates the regime where NFL behavior has been detected.

increase of C_{4f}/T can be observed for temperatures $0.3<T<4$ K for $x=0.95$, $0.5<T<5$ K for $x=0$ and $0.3<T<10$ K in $y=0.1$. However, while this NFL enhancement amounts to only 30% for $y=0$ and $y=0.1$, the specific-heat coefficient is almost enhanced by a factor of 3 for $x=0.95$. Of course, at present we cannot exclude the possibility that $Ce(Pd_{1-x}Ni_x)_2Ge_2$ still reveals magnetic order below 0.3 K. However, for three compounds we find a logarithmic increase at least over one decade in temperature which usually is taken as experimental evidence for a pure regime and not for a crossover behavior.

IV. ANALYSIS OF THE EXPERIMENTAL RESULTS AND DISCUSSION

A. Doniach-type phase diagram

First of all, from these experiments we tried to construct a Doniach-type phase diagram of the complete series of alloys that have been investigated in the course of this work. We tried to determine the characteristic Kondo-lattice temperatures from the low-temperature peak in the resistivity for the systems with weak hybridization (upper panel of Fig. 4) and from the maximum in the susceptibility for the strongly hybridized samples (lower panel of Fig. 2). Figure 9 shows the results as a function of the Ce-ligand distance r, which we treat as the relevant scaling parameter for the hybridization strength.[26,27] However, it has to be clearly stated that similar results would be obtained using the distance d or even the volume V. In addition, we plotted the AFM ordering temperatures in the palladium rich samples. Figure 9 clearly demonstrates that T^* increases strongly just at the critical concentration where magnetic order is suppressed. The shaded area shows the regime where NFL effects were detected.

B. Non-Fermi-liquid behavior

An important point of this work is the study of NFL phenomena close to the borderline from the magnetic order to a pure paramagnetic heavy-electron ground state. As we are close to a magnetic phase transition ($T_N \approx 0$ K at $x=0.9$) and at this concentration the alloys reveal only weak disorder we tried to compare our results with the predictions of the temperature dependence of the resistivity, susceptibility, and heat capacity close to a quantum critical point.[9,10] For a three-dimensional system with antiferromagnetic interactions, at the QCP we expect for the resistivity $\rho(T)=\rho_0+A'T^{3/2}$ and for the specific heat $C/T=\gamma_0-\alpha\sqrt{T}$ for temperatures $T\rightarrow 0$ K. At somewhat higher temperatures these laws show a crossover to $\rho \propto T$ and $C/T=\gamma_0' \ln(T_0'/T)$.

In a first step we analyzed the resistivity according to $\rho(T)=\rho_0+A'T^n$. We are aware that this procedure is a mere parameterization, but at present it is the only available model function. The solid lines in Fig. 5 show some of the representative results. From this figure it is immediately clear that power-law behavior in the different compounds is valid in restricted temperature ranges only. But that the deviations from the FL behavior are really significant is demonstrated in Fig. 6 where we plotted the deviations of the resistivity from a T^2 dependence below 2.5 K. We consistently used the same temperature range ($0.08<T<1.5$ K) to fit the resistivity data. The parameters of the fits to all experimental results using $\rho(T)=\rho_0+A'T^n$ are shown in Fig. 10. Here we plotted the temperature exponent n and the prefactor A' as a function of the Ce-transition metal distance r. Clear deviations from FL behavior appear close to the critical concentration. At high-Si concentrations, in the IV regime, pure FL behavior is observed, with an exponent $n=2$ and a small prefactor A'. In the magnetically ordered regime we found $n=2.3$ and again a small prefactor. The exponent is significantly larger than 2 is due to the scattering of charge carriers by magnetic excitations. Close to the critical regime $n=1.5\pm0.2$ in accordance with the predictions of the theory of a QCP.

In a similar way in Fig. 11 we plotted the r dependence of the specific-heat coefficient γ. We did not attempt to plot values for $x=0.9$ and $x=0.95$, which definitely would lie

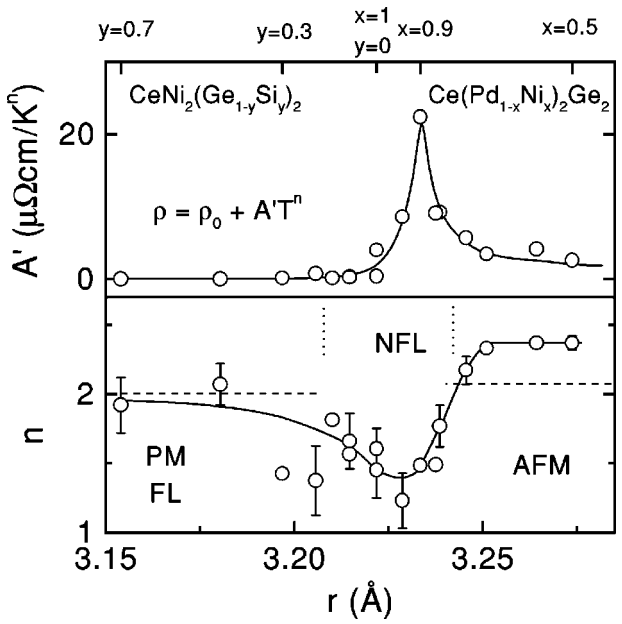

FIG. 10. The prefactor A' and the temperature exponent n as a function of r, the distance between the Ce and the transition-metal ion.

above 1 J/mole K^2. All quantities plotted in Figs. 10 and 11 show an extremum close to x_c. However, the temperature exponent n of the anomalous scattering extends far into the IV regime.

The relevant result of the heat capacity was given in Fig. 8. Here we showed the magnetic part of the heat capacity C_{4f}/T vs $\log(T)$. We find a logarithmic increase in the specific-heat coefficient, as it is found in many systems, while the theories predict a square-root dependence for a system with AFM interactions at lowest temperatures.[9,10] E.g., in the paramount example $CeCu_{6-x}Au_x$ on decreasing temperatures, also a logarithmic increase of the specific-heat coefficient has been detected, together with a linear decrease of the resistivity.[25] In this case the experimental findings have been explained assuming two-dimensional magnetic fluctuations[28] which also have been detected in neutron-scattering experiments.[29] In our case we have to assume, at least if the theories for a QCP are applicable for our system, that our heat-capacity experiments point towards a transition regime with a logarithmic dependence of the specific-heat coefficient in a limited temperature range.

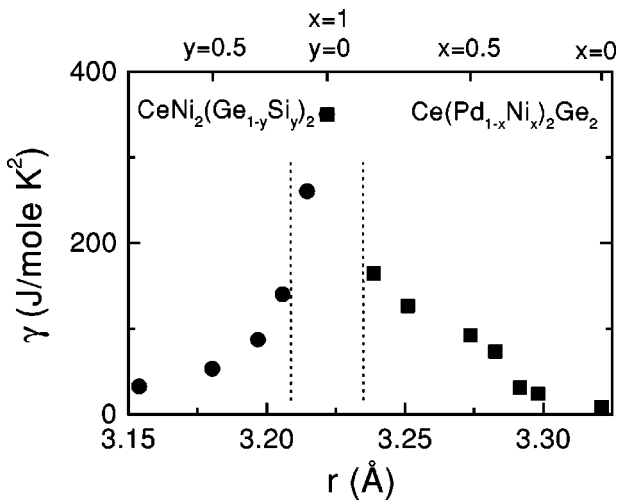

FIG. 11. Specific-heat coefficient γ as a function of r, the distance between the Ce and the transition-metal ion.

At this point it clearly has to be stated that in the same temperature region where the heat capacity increases logarithmically as a function of temperature, the resistivity follows a $T^{1.5}$ behavior, the true asymptotic temperature dependence at the QCP. In the crossover regime the resistivity is expected to reveal a linear temperature dependence. Similar discrepancies between specific heat and resistivity results were found in $CeCu_2Si_2$,[30] and have been reported $CeNi_2Ge_2$.[22] The following conclusions can be drawn from these findings: (i) The theory of a QCP is not strictly applicable to the systems investigated. And as the NFL behavior also governs the pure compound $CeNi_2Ge_2$ it is very unlikely that disorder scenarios (Griffiths phase or a distribution of Kondo temperatures) could explain these results. (ii) The different experimentally accessible quantities are not equally strongly influenced in the crossover regions which follow the asymptotic laws and/or are partly obscured by higher-order effects.

Astonishingly we find deviations from the Fermi-liquid behavior in a broad concentration regime around $CeNi_2Ge_2$ in the resistivity and in the specific heat. NFL behavior is also found in the $Ce(Cu_{1-x}Ni_x)_2Ge_2$ system for Ni concentrations $0.8<x<1$.[32–34] In Ref. 24 it is pointed out that $CeNi_2Ge_2$ is in the vicinity of a quantum critical point. They have studied different high-purity polycrystalline samples with extreme low residual resistances between 0.3 $\mu\Omega$ cm and 3 $\mu\Omega$ cm and they find a temperature dependence of the resistivity $\rho-\rho_0 \propto T^n$, where the size of the exponent $n \approx 1.4$ is lightly sample dependent. The sample with lowest residual resistivity has the lowest value $n=1.37$.[35] A similar relationship is found in the isostructural compound $CePd_2Si_2$.[36]

But we cannot exclude that the NFL behavior in the doped nonstoichiometric compounds is influenced by disorder effects. It has been shown that the NFL behavior in the $UCu_{1-x}Pd_x$ system can be calculated with a distribution of Kondo temperatures.[7] UCu_4Pd is a chemically ordered compound,[37] but, nevertheless, there is evidence for disorder from NMR and muon spin resonance measurements.[7] In the Kondo disorder model the temperature dependence of the resistivity is expected to be linear and while the specific-heat coefficient C/T follows logarithmic behavior.[8] However, our NFL system always reveals a power-law dependence in the resistivity with an temperature exponent $n>1.2$ and a logarithmic increase to low temperatures the specific-heat coefficient in the nonstochiometric compounds. For the pure system the specific-heat coefficient has a constant value $\gamma \approx 350$ mJ/mole K^2,[15,16] which is not consistent with the predictions of the Kondo-disorder model and indicates that Kondo disorder is not the dominant mechanism for the NFL behavior in the pure compound.

Finally, we only mention our measurements of the susceptibility. The susceptibility increases towards low temperatures, as theoretically predicted. However, we did not attempt to perform low-temperature measurements and also to carefully analyze our data. Presumably paramagnetic defects

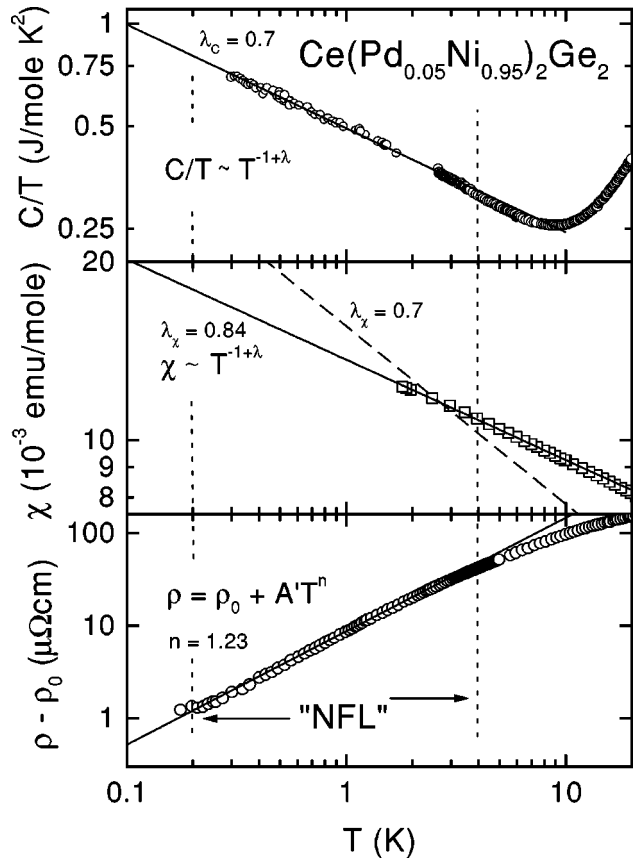

FIG. 12. $\log(C/T)$, $\log(\chi)$, and $\log(\rho-\rho_0)$ vs $\log(T)$ for $Ce(Pd_{0.05}Ni_{0.95})_2Ge_2$. The solid lines indicate the power laws yielding the best fit. It is not possible to fit susceptibility and specific-heat coefficient with one unique exponent. For the sake of clarity, a fit with the specific-heat exponent is indicated in the temperature dependence of the susceptibility.

hamper a precise analysis especially at very low temperatures. Furthermore, a detailed analysis of the polycrystalline samples is difficult due to the distinct anisotropy of the susceptibility, found in many HF compounds.

Very recently it has been proposed that most of the NFL results in HFS may be explained assuming the concept of a Griffiths phase. The Griffiths phase[13] is a cluster model of a spin glass. Of course, in metallic system which reveal a certain amount of disorder, a spin-glass phase is a natural consequence of this quenched disorder and the RKKY interaction which reveals sign changes as a function of spin-spin separations. For a Griffiths phase the specific-heat coefficient and the susceptibility are expected to reveal power laws $C(T)/T \propto \chi(T) \propto T^{-1+\lambda}$ with a unique and constant $\lambda < 1$ in the NFL regime.

In Fig. 12 we provide a test of our experimental results within the concept of the Griffiths phase. Here we plotted the logarithm of the specific-heat coefficient C/T, of the magnetic susceptibility $\chi(T)$, and of the resistivity $\rho(T)-\rho_0$, as a function of log (T) for $Ce(Pd_{0.05}Ni_{0.95})_2Ge_2$. The lines are fits with the theoretically predicted power laws. The best fits reveal for the specific heat $\lambda_C = 0.7$ and for the susceptibility $\lambda_\chi = 0.84$. It is not possible to describe both the specific heat and the susceptibility with the same value for λ. For the resistivity there exists no prediction up to now in the concept of the Griffiths phase. Also for the other concentrations, where NFL behavior is observed, it is not possible to describe the experimental data with one value for λ, too. We think that the existence of a Griffiths phase is not the origin of the NFL behavior in concentration regime around $CeNi_2Ge_2$, even if it is the only scenario, which predicts a NFL behavior in a broad concentration regime.

V. CONCLUSION

We have studied the Kondo-lattice compounds $Ce(Pd_{1-x}Ni_x)_2Ge_2$ and $CeNi_2(Ge_{1-y}Si_y)_2$ in the whole concentration regime. $CePd_2Ge_2$ is a local antiferromagnet with an ordering temperature of $T_N = 5.2$ K. With increasing Ni concentration x the hybridization between the $4f$ moments and the band states in $Ce(Pd_{1-x}Ni_x)_2Ge_2$ increases which leads to a suppression of the magnetic order for x close to 0.9. On diluting Ge by Si the hybridization strength further increases yielding IV compounds for high y concentrations. At the critical concentrations the characteristic temperatures (θ_p: Fig. 3; T^*: Fig. 9) show a strong noncontinuous increase. This is the regime where crystal electric-field (CEF) levels cease to exist as well-defined excitations. This can clearly be detected in the resistivity (Fig. 4), where the coherence peak ($T \approx 10$ K) and the CEF peak ($T \approx 75$ K) merge into one broad hump. It is also worth mentioning that CEF excitations have not been detected in $CeNi_2Ge_2$.[15] On doping with Cu the crystal field states evolve rapidly on decreasing hybridization.[38] In the region where the magnetism is suppressed, we found significant deviations from Fermi-liquid behavior in the electrical resistivity, the specific heat, and in the susceptibility in a rather broad concentration regime. These deviations cannot uniquely be explained with a distribution of Kondo temperatures or in the scenario of a Griffiths-phase singularity. Different power exponents λ have to be used for the specific-heat coefficient and for the susceptibility. Guided by the fact that in these alloys the quantum critical point appears close to the pure compound $CeNi_2Ge_2$ we feel that disorder plays a minor role and quantum critical phenomena should be observed. For temperatures $0.1 < T < 1.5$ the resistivity follows a power-law with an exponent $n \approx 1.5$ in accordance with the model predictions. However, in a similar temperature range ($0.3 \leqslant T \leqslant 5$ K) the specific-heat coefficient increases logarithmically towards low temperatures while a square-root dependence is expected. To test the predictions of the existence of a quantum critical point further measurements of the specific heat to lower temperatures are in progress.

ACKNOWLEDGMENT

This research was supported by the BMBF under Contract No. 13N6917/Elektronische Korrelationen und Magnetismus.

[1] G. R. Stewart, Rev. Mod. Phys. **56**, 755 (1984).
[2] N. Grewe and F. Steglich, *Handbook on the Physics and Chemistry of Rare Earth* (Elsevier Science Publishers B. V., Amsterdam, 1991), Vol. 14.
[3] S. Doniach, Physica B & C **91**, 231 (1977).
[4] H. v. Löhneysen, S. Mock, A. Neubert, T. Pietrus, A. Rosch, A. Schröder, O. Stockert, and U. Tutsch, J. Magn. Magn. Mater. **177-181**, 12 (1998); H. v. Löhneysen, F. Huster, S. Mock, A Neubert, T. Pietrus, O. Stockert, and M. Waffenschmidt, Physica B **230-232**, 550 (1997).
[5] D. L. Cox, Phys. Rev. Lett. **59**, 1240 (1987); D. L. Cox and M. Jarrel, J. Phys.: Condens. Matter **8**, 9825 (1996).
[6] P. Schlottmann and P. D. Sacramento, Adv. Phys. **42**, 641 (1993).
[7] O. O. Bernal, D. E. MacLaughlin, H. G. Lukefahr, and B. Andraka, Phys. Rev. Lett. **75**, 75 (1995); O. O. Bernal, D. E. MacLaughlin, A. Amato, R. Feyerherm, F. N. Gygax, A. Schenck, R. H. Heffner, L. P. Le, G. J. Niewenhuys, B. Andraka, H. v. Löhneysen, O. Stockert, and H. R. Ott, Phys. Rev. B **54**, 13 000 (1996).
[8] E. Miranda, V. Dobrosavljević, and G. Kotliar, J. Phys.: Condens. Matter **8**, 9871 (1996); Phys. Rev. Lett. **78**, 290 (1997).
[9] A. J. Millis, Phys. Rev. B **48**, 7183 (1993).
[10] T. Moriya and T. Takimoto, J. Phys. Soc. Jpn. **64**, 960 (1995).
[11] G. G. Lonzarich, in *Electron*, edited by M. Springford (Cambridge University Press, Cambridge, England, 1997).
[12] A. H. Castro Neto, G. Castilla, and B. A. Jones, Phys. Rev. Lett. **81**, 3531 (1998).
[13] R. B. Griffiths, Phys. Rev. Lett. **23**, 17 (1969).
[14] M. J. Besnus, A. Essaihi, G. Fischer, N. Hamdaoui, and A. Meyer, J. Magn. Magn. Mater. **104-107**, 1387 (1992).
[15] G. Knopp, A. Loidl, K. Knorr, L. Pawlak, M. Duczmal, R. Caspary, U. Gottwick, H. Spille, F. Steglich, and A. P. Murani, Z. Phys. B **77**, 95 (1989).
[16] A. Loidl, A. Krimmel, K. Knorr, G. Sparn, M. Lang, C. Geibel, S. Horn, A. Grauel, F. Steglich, B. Weslau, N. Grewe, H. Nakotte, F. R. de Boer, and A. P. Murani, Ann. Phys. (Leipzig) **1**, 78 (1992).
[17] T. Fukuhara, S. Akamuru, T. Kuwai, J. Sakurai, and K. Maezawa, J. Phys. Soc. Jpn. **67**, 2084 (1998).
[18] E. V. Sampathkumaran and R. Vijayaraghavan, Phys. Rev. Lett. **56**, 2861 (1986).
[19] I. Das and E. V. Sampathkumaran, Phys. Rev. B **44**, 9711 (1991).
[20] G. Oomi, Y. Uwatoko, E. V. Sampathkumaran, and M. Ishikawa, Physica B **223** & **224**, 307 (1996).
[21] G. R. Stewart, Z. Fisk, J. O. Willis, and J. L. Smith, Phys. Rev. Lett. **52**, 679 (1984).
[22] F. Steglich, B. Buschinger, P. Gegenwart, M. Lohmann, R. Helfrich, C. Langhammer, P. Hellmann, L. Donnevert, S. Thomas, A. Link, C. Geibel, M. Lang, G. Sparn, and W. Assmus, J. Phys.: Condens. Matter **8**, 9909 (1996); F. Steglich, P. Gegenwart, R. Helfrich, C. Langhammer, P. Hellmann, L. Donnevert, C. Geibel, M. Lang, G. Sparn, W. Assmus, G. R. Stewart, and A. Ochiai, Z. Phys. B **103**, 235 (1997).
[23] J. D. Thompson, Y. Uwatoko, T. Graf, M. F. Hundley, D. Mandrus, C. Godart, L. C. Gupta, P. C. Canfield, M. Migliori, and H. A. Borges, Physica B **199** & **200**, 589 (1994).
[24] O. Trovarelli, M. Weiden, R. Müller-Reisener, M. Gomez-Berisso, P. Gegenwart, M. Deppe, C. Geibel, J. G. Sereni, and F. Steglich, Phys. Rev. B **56**, 678 (1997).
[25] H. v. Löhneysen, T. Pietrus, G. Portisch, H. G. Schlager, A. Schröder, M. Sieck, and T. Trappmann, Phys. Rev. Lett. **72**, 3262 (1994); H. v. Löhneysen, J. Phys.: Condens. Matter **8**, 9689 (1996).
[26] A. Loidl, K. Knorr, G. Knopp, A. Krimmel, R. Caspary, A. Böhm, G. Sparn, C. Geibel, F. Steglich, and A. P. Murani, Phys. Rev. B **46**, 9341 (1991).
[27] J. Sereni and O. Trovarelli, J. Magn. Magn. Mater. **140-144**, 885 (1995).
[28] A. Rosch, A. Schröder, O. Stockert, and H. v. Löhneysen, Phys. Rev. Lett. **79**, 159 (1997).
[29] A. Schröder, G. Aeppli, E. Bucher, R. Ramazashvili, and P. Coleman, Phys. Rev. Lett. **80**, 5623 (1998); O. Stockert, H. v. Löhneysen, A. Rosch, N. Pyka, and M. Loewenhaupt, *ibid.* **80**, 5627 (1998).
[30] P. Gegenwart, C. Langhammer, C. Geibel, R. Helfrich, M. Lang, G. Sparn, F. Steglich, R. Horn, L. Donnevert, A. Link, and W. Assmus, Phys. Rev. Lett. **81**, 1501 (1998).
[31] P. Hellmann, L. Donnevert, S. Thomas, C. Geibel, G. Sparn, and F. Steglich, Czech. J. Phys. Suppl. 5 **46**, 2591 (1996).
[32] N. Büttgen, R. Böhmer, A. Krimmel, and A. Loidl, Phys. Rev. B **53**, 5557 (1996).
[33] G. Knebel, C. Eggert, T. Schmid, A. Krimmel, M. Dressel, and A. Loidl, Physica B **223** & **224**, 593 (1996).
[34] F. Steglich, P. Gegenwart, C. Geibel, R. Helfrich, P. Hellmann, M. Lang, A. Link, R. Modler, G. Sparn, N. Büttgen, and A. Loidl, Physica B **223** & **224,** 1 (1996).
[35] G. Sparn, L. Donnevert, P. Hellmann, F. Laube, A. Link, S. Thomas, P. Gegenwart, B. Buschinger, C. Geibel, and F. Steglich, Rev. High Pressure Sci. Technol. **7**, 431 (1998).
[36] F. M. Grosche, S. R. Julian, N. D. Mathur, and G. G. Lonzarich, Physica B **223** & **224**, 50 (1996).
[37] R. Chau, M. B. Maple, and R. A. Robinson, Phys. Rev. B **58**, 139 (1998).
[38] A. Krimmel, A. Loidl, and A. Severing, J. Phys.: Condens. Matter **9**, 873 (1997).